Journal of Molecular Structure 1223 (2021) 129193

Contents lists available at ScienceDirect

Journal of Molecular Structure

journal homepage: www.elsevier.com/locate/molstr

Substitutional effects on the reactivity and thermal stability of dihydropyrimidinones

Rasheed A. Adigun[a], Frederick P. Malan[a], Mohammed O. Balogun[b], Natasha October[a,*]

[a] Department of Chemistry, University of Pretoria, Lynnwood Road, Hatfield, Pretoria, 0002, South Africa
[b] Biopolymer Modification & Therapeutics Laboratory, Chemicals Cluster, Council for Scientific and Industrial Research, Meiring Naude Road, Brummeria, Pretoria 0001, South Africa

ARTICLE INFO

Article history:
Received 9 May 2020
Revised 31 August 2020
Accepted 1 September 2020
Available online 2 September 2020

Keywords:
Dihydropyrimidinone
Azide formation
Differential scanning calorimetry
Thermogravimetric analysis
Nucleophilic substitution
DFT study

ABSTRACT

One of the advantages of dihydropyrimidinones (DHPMs) is the molecular diversity that could be achieved through their synthesis from a three-component reaction by varying the starting reaction materials. Differences in substituted functional groups could lead to varying reactivities and thermal stability amongst the analogues. In this study, two different classes of DHPMs were synthesized and the effects of the various substituents on the DHPM ring were investigated. The compounds were structurally characterized using single-crystal X-ray diffractometry, ^{1}H, ^{13}C, COSY, HSQC and HMBC NMR techniques, FT-IR and High Resolution Mass Spectrometry (HRMS). N1 methylation of the DHPM was found to increase the thermal stability of the series of DHPMs investigated, which is an added advantage in thermal reactions. The nature of the alkyl substituent of the ester group at position 5 of the DHPM was also found to affect the ease of the nucleophilic substitution reaction during the functionalization of the DHPMs. A complementary DFT study aided in understanding the above results as well as to compare the general stability of the range of compounds.

1. Introduction

Dihydropyrimidinones (DHPMs) derived from the Biginelli multicomponent reaction (MCR) have attracted interests since the early 1980s due to their structural similarity to the well-studied dihydropyrimidine (DHP)-based calcium channel inhibitors (CCI) such as Amlodipine and Nifedipine [1–3]. It has been established that, apart from other therapeutic properties they possess [1], DHPMs share a similar therapeutic profile to DHP CCIs [2–5].

Complex molecules could be strategically synthesized by applying the basic knowledge of a two-component reaction, but this is usually time-consuming [6]. Multicomponent reaction (MCR) is a useful tool in this regard as it can selectively generate diverse chemical libraries on a short time scale [6]. As MCRs involve the use of more than two starting reaction materials, it is possible to strategically vary one material, to generate a library of various chemical compounds [6,7].

With the rise in cancer cases [8,9] in Africa and continued prevalence of the historically endemic malaria [10], there is a potential therapeutic challenge of having to treat, simultaneously, patients bearing “a double burden of diseases” [11]. There is a risk of drug-drug interactions from the current separate chemotherapeutic agents used in the treatment regimens of cancer and malaria [12]. One alternative option would be to use hybrid drugs [13]. Since DHPMs are known for their anticancer activities [14], this class of compounds can be synthesised with a chlorine atom at position 6 of the DHPM, which could easily be converted to an azide. An azide is a key reactive functional group in click chemistry that can be further employed to link a known antimalarial compound. In addition, the chloro precursor could be utilized in cyclization reactions to form fused heterocyclic systems to generate different biologically active libraries.

Previous studies on the functionalization of the halogenated DHPM reported the use of bromo and chloro analogues while, to the best of our knowledge, nothing could be found on how the ester substituents at the position 5 of the DHPM affect the ease of the functionalization [15,16]. Similarly, the previously reported thermal stability studies were carried out on DHPM with unsubstituted urea analogues but nothing could be found on how the alkyl substituents on the urea affect the thermal stability of the chloro DHPM [15,16]. We describe here the syntheses of dihydropyrimidinone-containing alkyl chlorides and functionalize them as the corresponding alkyl azides to yield useful precursors for click chemistry as part of ongoing research to synthesise biologically active dihydropyrimidinone-containing triazole

* Corresponding author.
E-mail address: natasha.october@up.ac.za (N. October).

https://doi.org/10.1016/j.molstruc.2020.129193
0022-2860/

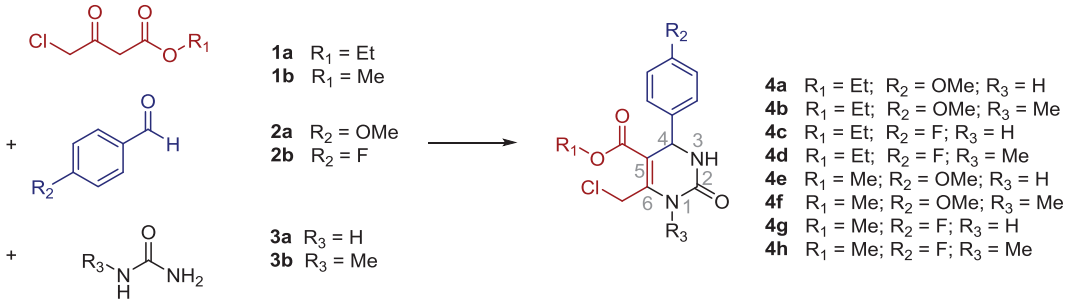

Scheme 1. Synthesis of the DHPM **4a-h**. Reagents and conditions: Conc. HCl (32%), absolute EtOH, reflux (65 °C), 3 h.

Table 1
^{1}H and ^{13}C chemical shifts (in ppm) of compound **4a**.

No	^{1}H	^{13}C	No	^{1}H	^{13}C
C_1	4.59 (1H, d, $^{2}J_{HH}$ = 10.7 Hz), 4.76 (1H, d, $^{2}J_{HH}$ = 10.6 Hz)	39.9	C_8	4.03 (2H, q, $^{3}J_{HH}$ = 7.1 Hz)	60.5
N_1	9.47 (1H, s)		C_9	1.12 (3H, t, $^{3}J_{HH}$ = 7.1 Hz)	14.4
C_2		152.6	C_{10}		136.5
N_3	7.79 (1H, s)		$C_{11,15}$	7.16 (2H, d, $^{3}J_{HH}$ = 8.5 Hz)	128.0
C_4	5.14 (1H, d, $^{3}J_{HH}$ = 3.3 Hz)	53.7	$C_{12,14}$	6.89 (2H, d, $^{3}J_{HH}$ = 8.5 Hz)	114.3
C_5		102.6	C_{13}		159.1
C_6		146.1	C_{16}	3.72 (3H, s)	55.5
C_7		164.7			

compounds. Additionally, the effect of the alkyl substituent on the thermal stability of DHPM was carried out to establish the optimum temperature which could be used during cyclization reactions.

2. Results and discussion

2.1. Synthesis of the DHPMs

The dihydropyrimidones **4a-h** were synthesized *via* an HCl-catalysed three-component Biginelli reaction as previously reported in the literature but with simple modifications using the appropriate benzaldehyde, urea and alkyl 4-chloroacetoacetate (Scheme 1) [1,17]. In the previous procedure involving HCl as the catalyst, the reaction mixture was stirred in neat condition at 100 °C. In this case, the reaction temperature was lowered to 65 °C while using absolute ethanol as the reaction solvent. After the completion of the reaction, the mixture was then placed in crushed ice overnight to afford the crude products as microcrystalline precipitates. The precipitates formed were filtered, washed with cold water and recrystallized from hot ethanol to afford pure products.

2.2. NMR characterization

Compound **4a** was chosen as a representative example for a comprehensive NMR characterization using ^{1}H, ^{13}C, DEPT-135, COSY, HSQC and HMBC techniques. For a summary of the ^{1}H and ^{13}C assignments (from HSQC and HMBC spectra), see Table 1. The numbering used is based on the SCXRD diagram of **4a** in Fig. 1. From the ^{1}H NMR of **4a**, the 3H ($^{3}J_{HH}$ = 7.1 Hz) triplet at δ_H 1.12 ppm, the 2H ($^{3}J_{HH}$ = 7.1 Hz) quartet at δ_H 4.03 ppm and the 3H singlet at δ_H 3.72 ppm were assigned to C(9)H_3, C(8)H_2 and the methoxy at C16, respectively. This was based on their multiplicity, coupling constants and the strong COSY correlation between the peaks at δ_H 1.12 ppm and 4.03 ppm. The signals for the methylene protons C(1)H_2 appeared as two doublets at δ_H 4.59 ($^{2}J_{HH}$ = 10.7) and 4.76 ($^{2}J_{HH}$ = 10.6) ppm and were assigned to C(1)H_2. The two doublets for the two geminal methylene protons at C6 were attributed to the enantiomeric nature of the compounds [18,19]. The assignment was supported by their strong correlation in the COSY spectrum. Furthermore, a doublet appearing at δ_H 5.14 ppm ($^{3}J_{HH}$ = 3.3 Hz), as well as a singlet at 9.47 ppm showed correlations in the COSY spectrum with the singlet at 7.79 ppm, while the singlet at 7.79 ppm showed correlations to both signals at 5.14 and 9.47 ppm. Therefore, δ_H 5.14, 7.79 and 9.47 ppm were assigned to C(4)*H*, N(3)*H* and N(1)*H*, respectively. Expectedly, the aromatic protons at δ_H 6.89 (d, $^{3}J_{HH}$ = 8.5 Hz) and 7.16 ppm (d, $^{3}J_{HH}$ = 8.5 Hz) have strong correlations in the COSY spectrum. In relation to the DFT section below (*vide infra*), the calculated ^{1}H and ^{13}C NMR spectra of selected compounds (**4a, 4e**, 4 h) have been considered (Figures S16-S21). In general, the relative ^{1}H NMR signals (corrected using TMS) shifts of between 0.1–2.0 ppm relative to the experimental signals were observed for each of the three compounds considered. The calculated ^{13}C NMR signals of corresponding compounds were more accurately predicted. For example, calculated signals for the carbonyl groups in **4a** at δ_C 166.7 and 163.8 ppm (and other signals) appeared within 0.1–13.7 ppm (up to 26% error) to those experimentally observed (calculated signals in brackets, δ_C): 164.7 (169.1), 159.1 (162.7), 152.6 (152.5), 146.1 (150.1), 136.5 (136.3), 128.0 (132.5), 114.3 for 2 carbons (120.4 and 111.5), 102.6 (106.4), 60.5 (65.8), 55.5 (59.9), 53.7 (59.4), 39.4 (53.1), 14.4 (15.4) ppm. Similar observations were also made with the calculated *versus* experimentally observed signals in the ^{13}C NMR spectra of compounds **4e** and 4 h.

2.3. Functionalization of the DHPMs

The C6 chlorine allowed the functionalization of the DHPMs with ease [16,20,21]. The C6 chlorine was attached *via* a chlorinated β-ketoester [16] used in the Biginelli MCR to explore how its functionalization could be affected by varying the alkyl group of the ester at position 5 of the DHPM (Scheme 1). The use of a chlorinated β-ketoester is synthetically more feasible than the tandem bromination [21,22] of the C6 methyl group using elemental bromine due to its notable stability, low cost and commercial availability [16].

To investigate the ease of their substitution, we substituted the chlorine in position 6 with an azide that would be used for further

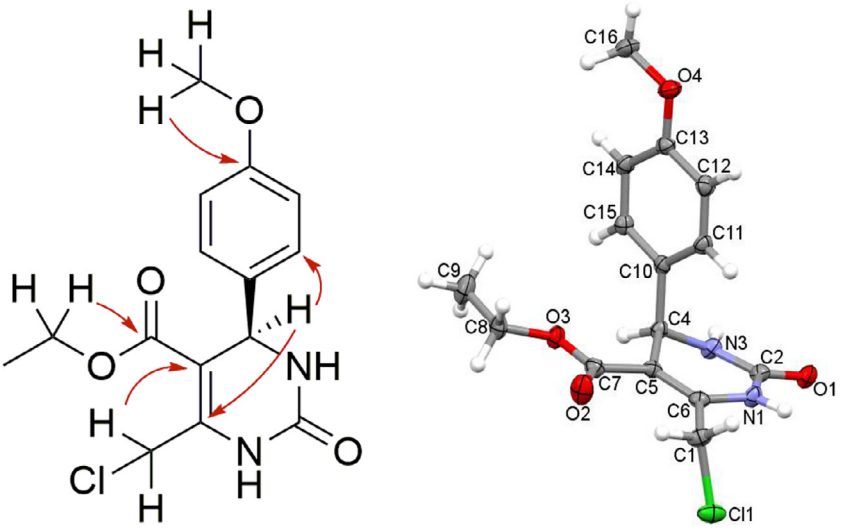

Fig. 1. Some HMBC correlations in compound **4a** and the molecular structure of **4a**.

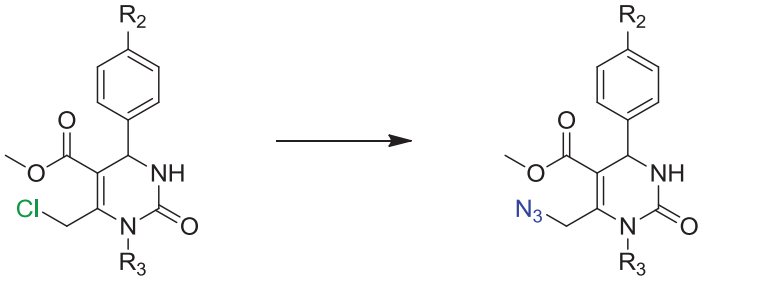

4e R_2 = OMe; R_3 = H
4f R_2 = OMe; R_3 = Me
4g R_2 = F; R_3 = H
4h R_2 = F; R_3 = Me

5e R_2 = OMe; R_3 = H
5f R_2 = OMe; R_3 = Me
5g R_2 = F; R_3 = H
5h R_2 = F; R_3 = Me

Scheme 2. Azidation reaction. Reagents and conditions: NaN_3, DMF, N_2, 6 h, 25 °C.

derivatization in click reactions [20,22]. We assessed the ease of the azidation by stirring the DHPMs in DMF at 25 °C in the presence of approximately one molar equivalent of sodium azide only. Previous methods with similar compounds involved the use of catalysts [20], long hours of stirring in hexamethylorthophosphoric triamide (HMPA) [23] or microwave irradiation [20]. Interestingly, compounds **4e-h** with a methyl group produced the corresponding azides in near quantitative yields (Scheme 2) whereas compounds **4a-d** with an ethyl group failed to be converted to the corresponding azides even at an elevated temperature and prolonged stirring.

The reaction was monitored by Fourier transform infrared spectroscopy (FT-IR) and the presence of the azide functional group was confirmed with the absorption band around 2100 cm^{-1} (Fig. 2).

As an example, we compared the ^1H NMR of 4 g and 5 g (Fig. 3), and observed a change in the δ_H value of C(1)H_2 from δ_H 4.66 ppm in 4 g to δ_H 4.40 ppm in 5 g, which indicated an upfield shift [24] due to the presence of the electron-donating azide group. In the same way, the ^{13}C peak of *C*(1) also shifted from δ_C 39.7 ppm in 4 g to 48.5 ppm in 5 g [24].

2.4. X-ray crystallography

Apart from the unambiguous confirmation of the presence of the azide group in compounds **5e-h**, the respective structural changes that occurred from the conversion of the alkyl chloride to the alkyl azide were investigated by SCXRD (Fig. 4). The X-ray crystallography of all the structures from both the alkyl chloride and alkyl azide series confirmed their racemic nature by crystallising in the centrosymmetric space groups of *P*-1 (**4a-c, 5f**, 5 g), $P2_1/n$ (**4d**), $P2_1/c$ (**4f**), and *C*2/*c* (5 h). All structures exhibited only one chiral centre at C4 and likewise, a distorted half-chair conformation was observed with the heterocycle mean plane through the five coplanar atoms (N3-C2-N1-C6-C5) intersecting at *ca.* 22.5°–43.9° with the mean plane of the N3-C4-C5 inclined-section of the heterocycle. A general trend amongst these distortions was observed for the NMe-substituted heterocycles (**4b, 4d, 4f, 5f**, 5 h) which exhibited larger intersection angles (28.6°–43.9°) as compared to the NH-substituted heterocycles (**4a, 4c**, 5 g) (22.5°–23.4°). Interestingly in all the structures, the aryl groups occupy the axial position even though large, bulky substituents of cyclohexanes in the corresponding chair conformations usually occupy the equatorial positions. No apparent steric hindrance of 1,3-diaxial repulsion could be observed due to the planar nature of the heterocycle (C_{arene}-C4-H4 angle between 107.52°–108.30°). Therefore, the fact that the alkyl chloride/azide chain occupies the *trans* position to that of the aryl group, as well as favourable intermolecular interactions in the solid state, could be seen as a determining factor. However, this conformation is free to oscillate while in solution to a more energetically favourable conformer. Within all of the structures, the mean plane of the pyrimidinone ring intersects the mean plane of the para-substituted arene on C4 in a narrow range of between 79.0° (**4f**) and 89.37° (5 g). Other minor differences amongst the

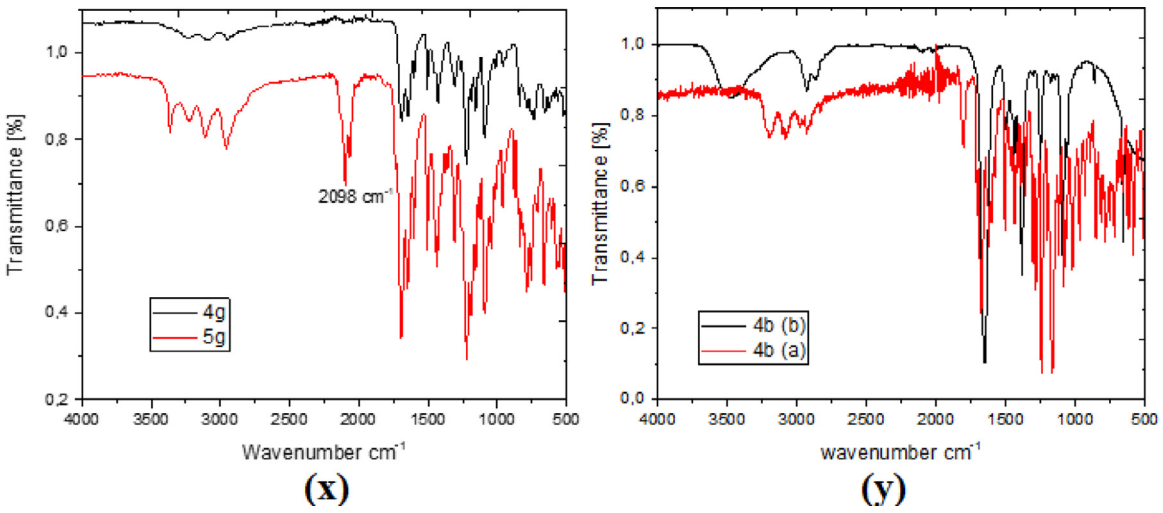

Fig. 2. (**x**): The FT-IR of 4 g and 5 g. The peak at 2098 cm^{-1} indicates the azide absorption. (**y**): The FT-IR of **4b** before (a) and during the azidation reaction (b) taken *in situ*.

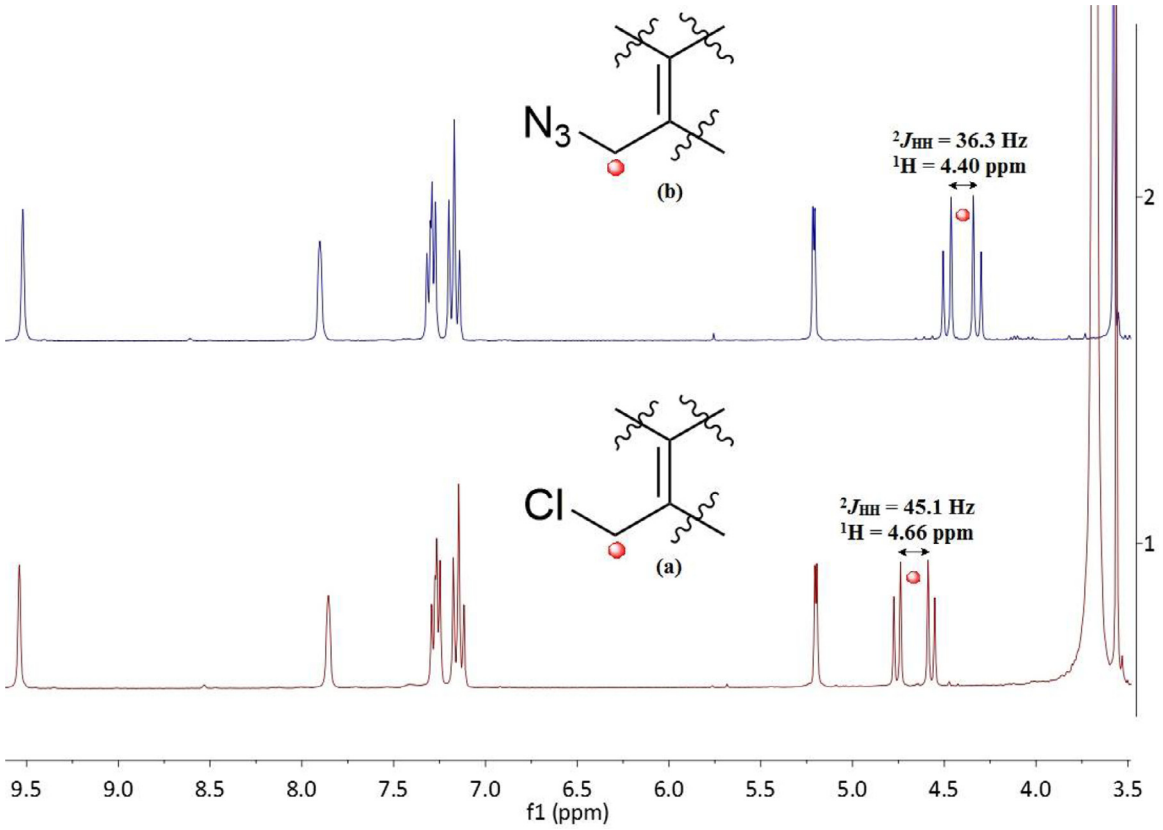

Fig. 3. ^{1}H NMR of 4 g (a) and 5 g (b) indicating the *J*-coupling constants and the chemical shifts of C(7)H_2 as a result of the azidation reaction (300 MHz, DMSO–d_6).

different structures include a narrow range for the C2-O1 bond distances (1.229(2)–1.238(2) Å), as well as the obvious C1-Cl and C1-N_3 bond distance differences (X = Cl: 1.7873(16)–1.8080(18) Å; X = N_3, 1.482(2)–1.488(3) Å). In all structures, strong intermolecular N–H•••O hydrogen bonds (N–H•••*O* = 1.962 Å, 173.1°) form molecular dimers with two pyrimidinone molecules and also link these dimers *via* other N–H•••O and weaker C–H•••Cl interactions to extend into a three-dimensional network. All other bond lengths and angles are observed to fall within the expected ranges and are in good agreement with related structures [25–27].

2.5. DFT study of the alkyl chlorides and azide DHPMs

To gain more insight into the substituent effect(s) that direct the ease and outcome of the azidation reactions of the alkyl chloride compounds **4a-h** to produce compounds **5e-h**, as well as to gain a general understanding of the consequent racemic nature of all the compounds, a Density Functional Theory (DFT) computation study was performed. In general, input structures were obtained from the crystallographic information files (CIFs) and further optimized until conversion with zero imaginary frequencies. In all the structures, a relatively small energy difference of between 0.0045

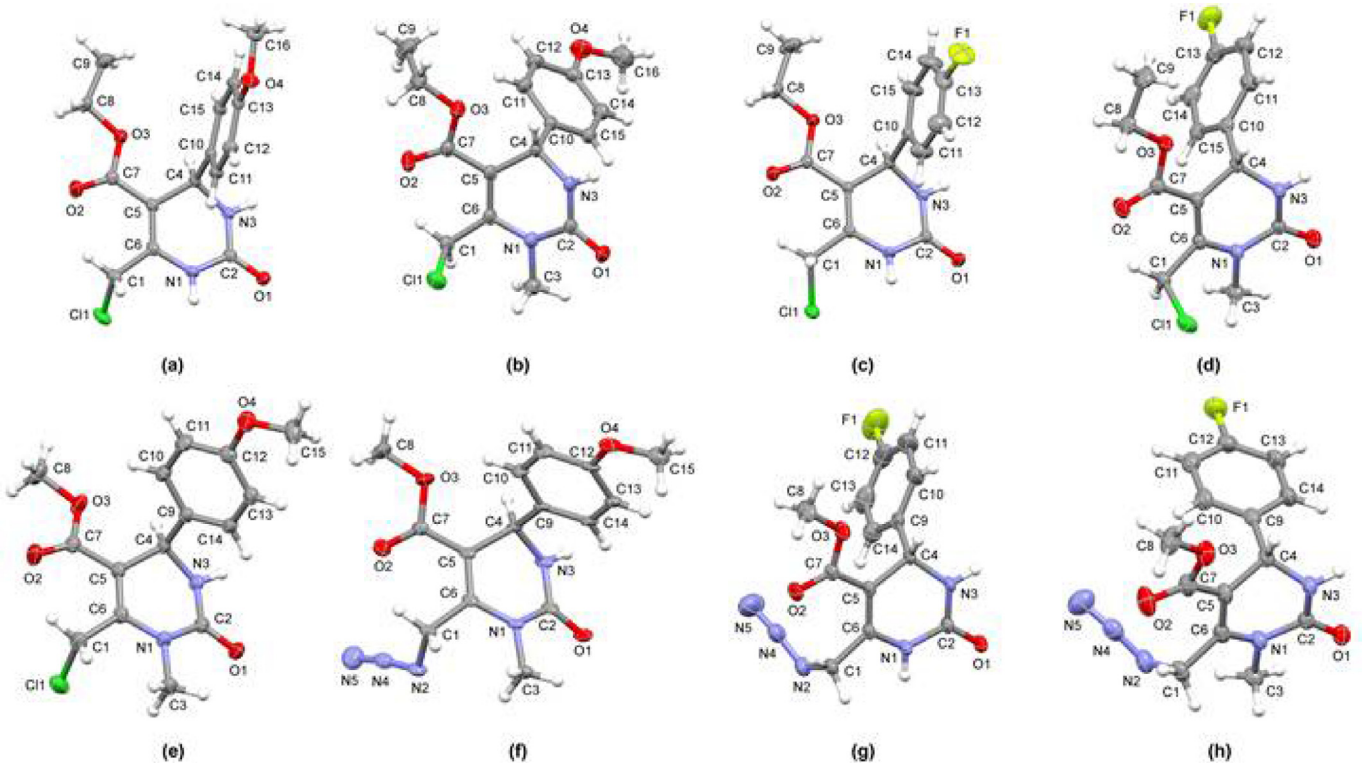

Fig. 4. Perspective views of the molecular structures of **4a** (a), **4b** (b), **4c** (c), **4d** (d), **4f** (e), **5f** (f), 5 g (g), and 5 h (h). Thermal ellipsoids are drawn at 50% level.

Table 2
Calculated relative Gibbs free energies (eV) and orbital energies for the different isomers of compound **4a-h**, and **5e-h**.

Compound	Functional groups Alkyl chloride/azide	Ester	R2	R3	Relative *E* (eV)	Isomer	Energy gap (eV)
4a	chloride	COOEt	OMe	H	**0.0000**	***R***	−4.49
					0.0072	*S*	
4b	chloride	COOEt	OMe	Me	0.0129	*S*	−4.31
					0.0000	***R***	
4c	chloride	COOEt	F	H	**0.0000**	***R***	−4.85
					0.0045	*S*	
4d	chloride	COOEt	F	Me	**0.0000**	***S***	−4.55
					0.0557	*R*	
4e	chloride	COOMe	OMe	H	**0.0000**	***R***	−4.49
					0.0214	*S*	
4f	chloride	COOMe	OMe	Me	0.0077	*R*	−4.35
					0.0000	***S***	
4 g	chloride	COOMe	F	H	**0.0000**	***R***	−4.85
					0.0053	*S*	
4h	chloride	COOMe	F	Me	0.0096	*R*	−4.55
					0.0000	***S***	
5e	azide	COOMe	OMe	H	0.0077	*R*	−4.75
					0.0000	***S***	
5f	azide	COOMe	OMe	Me	0.0194	*R*	−4.46
					0.0000	***S***	
5 g	azide	COOMe	F	H	0.0339	*R*	−4.94
					0.0000	***S***	
5h	azide	COOMe	F	Me	**0.0000**	***R***	−4.71
					0.0267	*S*	

Values in bold indicate the lowest calculated energy enantiomer.

and 0.0557 eV was observed for all stereoisomers of all compounds (Table 2). This implies that both isomers can experimentally exist, as has been established by SCXRD.

Shown in Fig. 5 are the HOMO and LUMO orbital plots. The general populations of the HOMOs and LUMOs of both the alkyl chlorides (**4a-h**) and alkyl azides (**5e-h**) are comparative as follows: (i) The HOMO of **4a, 4e** and **5e,** differing only in the chloride/azide functional groups, shows the major contribution from the arene groups on C4, whereas the LUMO of **4a, 4e** and **5e** shows a shift in contribution towards both the ester functional group, as well as C6. Interestingly, no LUMO contribution on the CH_2N_3-group of **5e** is present in contrast to the CH_2Cl-group of either the methoxy derivative **4e** or ethoxy derivative **4a**, despite **5e** being considered as the more reactive analogue; (ii) Upon substitution of the 4′-OMe group for a 4′-F group, the distribution of the HOMOs of both 4 h and 5 h, which are chloride and azide-containing groups, re-

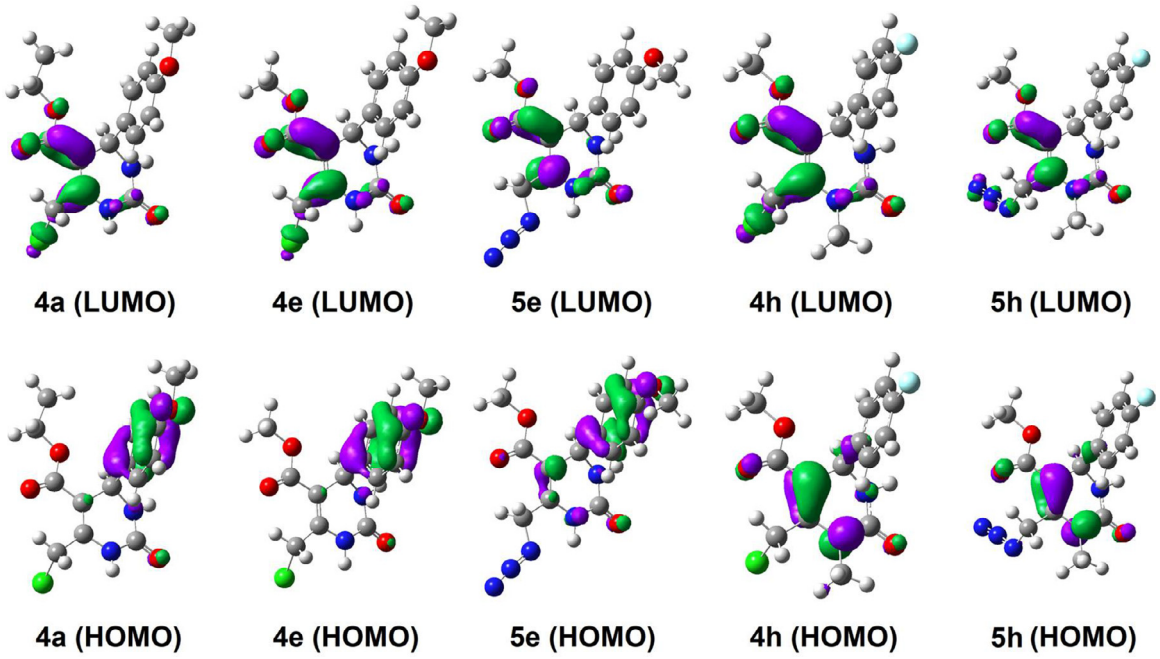

Fig. 5. Frontier orbitals of selected alkyl chloride (**4a, 4e**, 4 h) and alkyl azide (**5e**, 5 h) compounds.

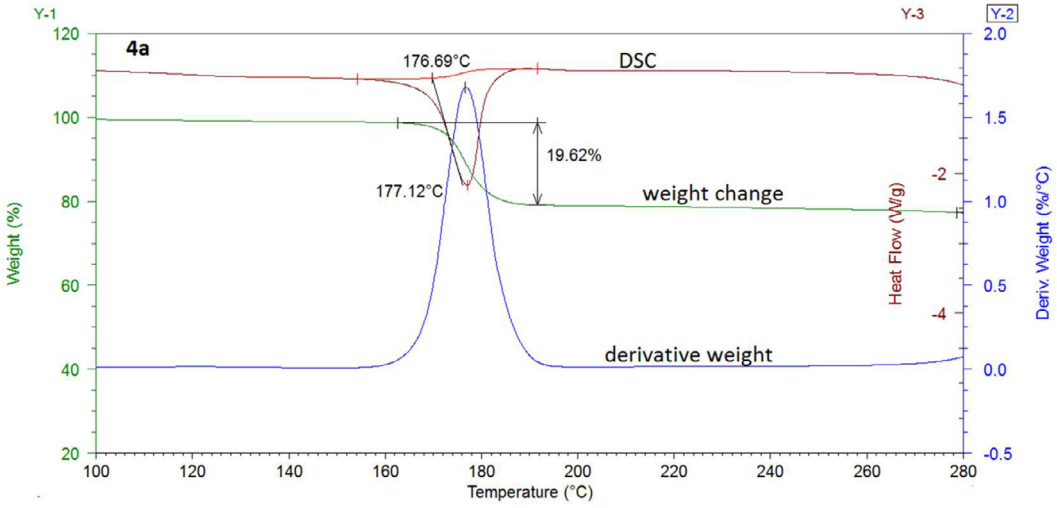

Fig. 6. TGA-DSC thermogram of **4a**.

spectively, shifts completely away from the arene groups on C4 to rather include the pyrimidinones backbone atoms of N1, C5 and C6. The LUMOs of 4 h and 5 h, however, are relatively comparable with the LUMOs of **4a, 4e** and **5e**, i.e. the 4′-OMe-containing arene groups.

In general, an expected increase in energy of around 8 keV is observed upon substitution of the chloride group for a more reactive azide functional group. This is sensible when considering the energy gaps of the alkyl chloride and corresponding alkyl azide compounds: a decrease of between 0.09 eV and 0.26 eV is seen upon substitution of the chloro group in compounds **4e-h** to form compounds **5e-h**. Interestingly, a noticeable increase in energy gap and therefore the stability of the molecule is seen in analogous examples upon substitution of a 4′-OMe group for a 4′-F group. Depending on the other substituents, a decrease of between 0.24 eV (**4b** and **4d**) and 0.35 eV (**5e** and 5 g) is observed. The current available data is insufficient to convincingly explain the reduced reactivities of compounds **4a-4d** with COOEt groups when the conversion to their analogous azide counterparts was attempted. Additional natural bond orbital (NBO) interactions were evaluated as part of the DFT studies to observe any interaction involving the chlorine, ester and arene groups, although no significant interactions of the donor/acceptor atom orbitals were observed.

2.6. Thermal stability study of compounds 4a-d

The effect of the N1 methylation on the thermal stability of compounds **4a-d** was studied using Differential Scanning Calorimetry (DSC) and Thermogravimetric Analysis (TGA). As mentioned earlier, the C6 alkyl chloride could be used to access some molecular transformations that include thermal ring closures and rearrangements [16,28,29]. Since such reactions are normally carried out at high temperatures, it is necessary to carefully analyse their thermal properties in order to choose an optimum reaction temperature to avoid decomposition of reactants. The melting points of **4a-d** were determined and found to be in close agreement with

Table 3
Thermal analysis of **4a-d**.

Compound	MP[a] (°C)	MP[b] (°C)	OT[b] (°C)	MP[c] (°C)	FD (°C)	WL (%)	CS Lost
4a	172–174	177.85	173.65	177.12	176.69	19.62	urea
4b	141–143	141.55	138.53	141.35	250.01	34.19	benzaldehyde
4c	154–157	159.24	155.02	158.41	163.93	17.77	urea
4d	158–160	161.04	158.14	159.74	252.6	34.21	benzaldehyde

MP = melting point, OT = onset temperature, FD = first decomposition, WL = weight loss, CS = corresponding synthon.
[a] = Gallenkamp.
[b] = DSC.
[c] = TGA-DSC.

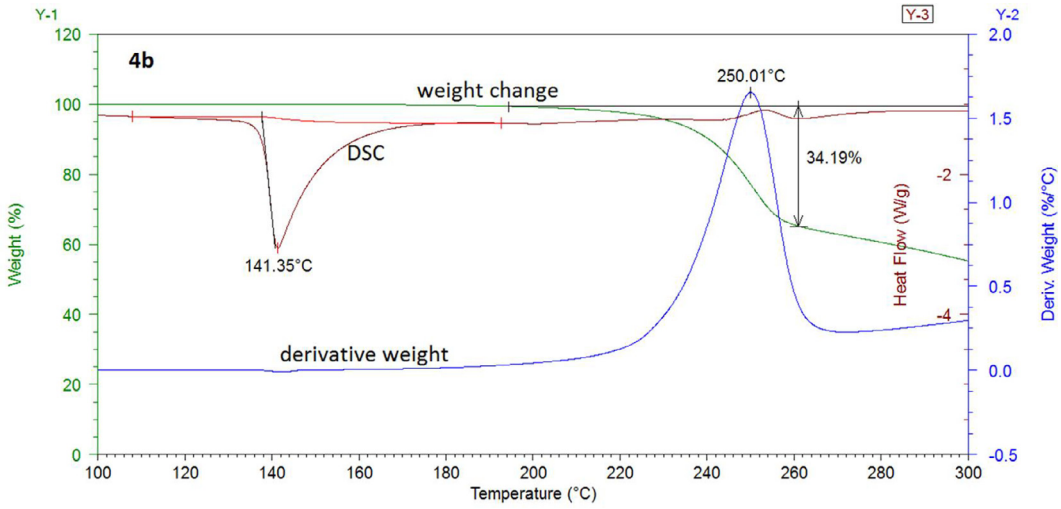

Fig. 7. TGA-DSC thermogram of **4b**.

the melting temperatures obtained from DSC studies (Table 3). The DSC thermogram obtained involved initial heating from −20 °C to 250 °C at the rate of 10 °C/min under a nitrogen purge with a flow rate of 10.0 mL/min. This was followed by a slow cooling and then the second heating. The only melting obtained on the DSC thermogram was in the first heating and no corresponding crystallization exotherm was observed on slow cooling. This DSC isotherm indicates a decomposition during heating after the melting temperature. To better understand the temperature-weight loss relationship, a TGA study was performed on all the four compounds. The TGA-DSC hyphenated thermograms showed the first weight loss at the melting point for compounds **4a** and **4c** at 176.69 and 163.93 °C, respectively which correspond to the initial melting points obtained from DSC (Table 3). Compounds **4b** and **4d** only showed the first weight loss at 250.01 °C and 252.60 °C, respectively, which is approximately a 100 °C difference between their melting points and the first weight loss (Figs. 6 and 7).

These results clearly show that the N1 methylation of **4b** and **4d** increases their thermal stability as compared to **4a** and **4c** without a methyl group at N1. Interestingly, both **4a** and **4c** lost 19.62 and 17.77 wt%, respectively, during the first decomposition, which corresponds to the urea synthon. **4b** and **4d** also lost 34.19 and 34.21 wt%, respectively, which corresponds to the benzaldehyde synthon in the DHPM. (See the SI for the full thermograms.) It can be concluded from these thermal analyses that **4a** and **4b** could safely withstand thermal reactions up to 150 °C while **4b** and **4d** could be heated up to 240 °C.

3. Conclusion

Two different classes of DHPM were synthesized, which differ in the ester substituent at position C5. This was found to be the primary contributor that influence the ease of nucleophilic substitution reaction involving the alkyl chloride at C6. During the nucleophilic reaction, compounds **4e**-**h**, with a methyl ester at C5, furnished the desired azide products at 25 °C without the use of any catalyst or microwave irradiation while azidation of compounds **4a-d** with ethyl ester failed, even at an elevated temperature and prolonged stirring. The formation of the azide product was monitored with FT-IR and its presence was established with further characterization. Although subtle energetic differences in the ester and aryl group substituents of **4a-h** could be established, no conclusive computational evidence could be provided for the lack of azide formation by compounds **4a-d**. The presence of the methyl group at N1 of the DHPM was also found to contribute to the thermal stability that was established using DSC and TGA.

4. Experimental

4.1. General

A Gallenkamp melting point apparatus was used for the melting point determination in open capillary tubes and are uncorrected. ^{1}H and ^{13}C NMR spectra were recorded on either a Bruker Avance 400 (at 400.21 MHz for ^{1}H and 100.64 MHz for ^{13}C) or 300 (at 300.13 MHz for ^{1}H and 75.48 MHz for ^{13}C) spectrometers using $CDCl_3$ or DMSO–d_6 as solvents at room temperature. Chemical shifts were recorded as part per million (ppm) using tetramethylsilane as an internal standard. 2D NMR experiments were recorded on Bruker Avance 400. Mass analysis was performed on Waters® Synapt G2 High Definition Mass Spectrometry (HRMS) system with flow injection analysis (FIA) using electrospray ionization (ESI) probe. The MS data were acquired and processed on MassLynx™ software (version 4.1). FT-IR measurements were made on a Bruker

Alpha Platinum-ATR spectrometer as neat. All reagents and solvents were purchased from Sigma-Aldrich and used without further purification. Differential scanning calorimetry (DSC) data were obtained using a TA DSC Q2000 analyser under a nitrogen atmosphere at a scan rate of 10 °C/min from −20 °C to 250 °C for the first heating. This was followed by a slow cooling to −20 °C at a rate of −20 °C/min and finally the second heating to 250 °C at a rate of 10 °C/min. Thermogravimetric analysis (TGA) data were obtained using a TA SDT Q600 analyser (DSC-TGA standard). The samples were heated up to 600 °C at a rate of 10 °C/min under a flow of nitrogen.

4.2. General procedure for the synthesis of tetrahydropyrimidine-5-carboxylates (**4a-h**)

To a mixture of the appropriate benzaldehyde (15.00 mmol), (m)ethyl 4-chloroacetoacetate (15.00 mmol) and urea or N-methylurea (45.00 mmol) in 10.0 mL ethanol was added 7 drops of concentrated HCl. The mixture was heated at 65 °C for 3 h. The resulting mixture was cooled to room temperature and further cooled in crushed ice overnight. The precipitate formed was filtered and recrystallized from hot ethanol to give the pure products.

Ethyl 6-(chloromethyl)−4-(4-methoxyphenyl)−2-oxo-1,2,3,4-tetrahydropyrimidine-5-carboxylate (**4a**): White crystals, Yield 83.6%. m.p. 172–174 °C. FT-IR: ν (cm^{-1}) = 3386 (N–H), 1680 (*C* = *O*, ester), 1643 (*C* = *O*, amide). ^{1}H NMR (400 MHz, DMSO–d_6): δ_H 9.47 (s, 1H, N*H*), 7.79 (s, 1H, N*H*), 7.16 (d, $^3J_{HH}$ = 8.5 Hz, 2H, Ar*H*), 6.89 (d, $^3J_{HH}$ = 8.5 Hz, 2H, Ar*H*), 5.14 (d, $^3J_{HH}$ = 3.3 Hz, 1H, C*H*), 4.76 (d, $^2J_{HH}$ = 10.6 Hz, 1H, CH_2), 4.59 (d, $^2J_{HH}$ = 10.7 Hz, 1H, CH_2), 4.03 (q, $^3J_{HH}$ = 7.1 Hz, 2H, CH_2CH$_3$), 3.72 (s, 3H, OCH_3), 1.12 (t, $^3J_{HH}$ = 7.1 Hz, 3H, CH$_2$CH_3). ^{13}C NMR (101 MHz, DMSO–d_6): δ_C 164.7, 159.1, 152.6, 146.1, 136.5, 128.0 (2C), 114.3 (2C), 102.6, 60.5, 55.5, 53.7, 39.9, 14.4. ESI-HRMS (*m/z*) calculated for $C_{15}H_{18}ClN_2O_4$: 325.0955, found: 325.0988 $[M + H]^+$.

Ethyl 6-(chloromethyl)−4-(4-methoxyphenyl)−1-methyl-2-oxo-1,2,3,4-tetrahydropyrimidine-5-carboxylate (**4b**): White crystals, Yield 93.2%. m.p. 141–143 °C. FT-IR: ν (cm^{-1}) = 3198 (N–H), 1679 (*C* = *O*, ester), 1623 (*C* = *O*, amide). ^{1}H NMR (400 MHz, $CDCl_3$): δ_H 7.16 (d, $^3J_{HH}$ = 8.7 Hz, 2H, Ar*H*), 6.82 (d, $^3J_{HH}$ = 8.7 Hz, 2H, Ar*H*), 5.77 (d, $^3J_{HH}$ = 3.3 Hz, 1H, N*H*), 5.35 (d, $^3J_{HH}$ = 3.2 Hz, 1H, C*H*), 4.93 (s, 2H, CH_2), 4.14 (q, $^3J_{HH}$ = 7.1 Hz, 2H, CH_2CH$_3$), 3.78 (s, 3H, OCH_3), 3.38 (s, 3H, NCH_3), 1.20 (t, $^3J_{HH}$ = 7.1 Hz, 3H, CH$_2$CH_3). ^{13}C NMR (101 MHz, $CDCl_3$): δ_C 164.8, 159.4, 153.6, 146.1, 134.7, 127.6 (2C), 114.2 (2C), 107.1, 60.9, 55.3, 53.4, 37.5, 29.4, 14.1. ESI-HRMS (*m/z*) calculated for $C_{16}H_{20}ClN_2O_4$: 339.1111, found: 339.1157 $[M + H]^+$.

Ethyl 6-(chloromethyl)−4-(4-fluorophenyl)−2-oxo-1,2,3,4-tetrahydropyrimidine-5-carboxylate (**4c**): White crystals, Yield 88.0%. m.p. 154–157 °C. FT-IR: ν (cm^{-1}) = 3356 (N–H), 1683 (*C* = *O*, ester), 1639 (*C* = *O*, amide). ^{1}H NMR (400 MHz, DMSO–d_6): δ_H 9.55 (d, $^3J_{HH}$ = 2.0 Hz, 1H, N*H*), 7.87 (dd, $^3J_{HH}$ = 3.4, 1.9 Hz, 1H, N*H*), 7.32 – 7.24 (m, 2H, Ar*H*), 7.21 – 7.13 (m, 2H, Ar*H*), 5.20 (d, $^3J_{HH}$ = 3.4 Hz, 1H, C*H*), 4.77 (d, $^2J_{HH}$ = 10.6 Hz, 1H, CH_2), 4.58 (d, $^2J_{HH}$ = 10.7 Hz, 1H, CH_2), 4.03 (qd, $^3J_{HH}$ = 7.1, 1.8 Hz, 2H, CH_2CH$_3$), 1.10 (t, $^3J_{HH}$ = 7.1 Hz, 3H, CH$_2$CH_3). ^{13}C NMR (101 MHz, DMSO–d_6) δ_C 164.6, 162.0 (d, $^1J_{CF}$ = 243.6 Hz), 152.4, 146.6, 140.6 (d, $^4J_{CF}$ = 3.0 Hz), 128.8 (2C, d, $^3J_{CF}$ = 8.4 Hz), 115.8 (2C, d, $^2J_{CF}$ = 21.3 Hz), 102.1, 60.5, 53.7, 14.3. ESI-HRMS (*m/z*) calculated for $C_{14}H_{15}ClFN_2O_3$: 313.0755, found: 313.0757 $[M + H]^+$.

Ethyl 6-(chloromethyl)−4-(4-fluorophenyl)−1-methyl-2-oxo-1,2,3,4-tetrahydropyrimidine-5-carboxylate (**4d**): White crystals, Yield 92.2%. m.p. 158–160 °C. FT-IR: ν (cm^{-1}) = 3351 (N–H), 1672 (*C* = *O*, ester), 1627 (*C* = *O*, amide). ^{1}H NMR (400 MHz, $CDCl_3$): δ_H 7.24 (dd, $^3J_{HH}$ = 8.6, $^4J_{HF}$ = 5.3 Hz, 2H, Ar*H*), 7.01 (t, $^3J_{HH,HF}$ = 8.7 Hz, 2H, Ar*H*), 6.21 (d, $^3J_{HH}$ = 3.4 Hz, 1H, N*H*), 5.41 (d, $^3J_{HH}$ = 3.4 Hz, 1H, C*H*), 5.00 (d, $^2J_{HH}$ = 11.9 Hz, 1H, CH_2), 4.92 (d, $^2J_{HH}$ = 11.8 Hz, 1H, CH_2), 4.17 (q, $^3J_{HH}$ = 7.1 Hz, 2H, CH_2CH$_3$), 3.40 (s, 3H, NCH_3), 1.22 (t, $^3J_{HH}$ = 7.2 Hz, 3H, CH$_2$CH_3). ^{13}C NMR (101 MHz, $CDCl_3$): δ_C 164.6, 162.5 (d, $^1J_{CF}$ = 246.9 Hz), 153.6, 146.6, 138.3 (d, $^4J_{CF}$ = 3.2 Hz), 128.1 (2C, d, $^3J_{CF}$ = 8.3 Hz), 115.8 (2C, d, $^2J_{CF}$ = 21.6 Hz), 106.8, 61.1, 53.2, 37.4, 29.5, 14.0. ESI-HRMS (*m/z*) calculated for $C_{15}H_{17}ClFN_2O_3$: 327.0912, found: 327.0944 $[M + H]^+$.

Methyl 6-(chloromethyl)−4-(4-methoxyphenyl)−2-oxo-1,2,3,4-tetrahydropyrimidine-5-carboxylate (**4e**) White solid, Yield 84.6%. m.p. 98–100 °C. FT-IR: ν (cm^{-1}) = 3223 (N–H), 1689 (*C* = *O*, ester), 1645 (*C* = *O*, amide). ^{1}H NMR (400 MHz, DMSO–d_6) δ_H 9.48 (d, $^4J_{HH}$ = 2.0 Hz, 1H, N*H*), 7.77 (t, $^{3,4}J_{HH}$ = 2.7 Hz, 1H, N*H*), 7.16 (d, $^3J_{HH}$ = 8.7 Hz, 2H, Ar*H*), 6.88 (d, $^3J_{HH}$ = 8.7 Hz, 2H, Ar*H*), 5.13 (d, $^3J_{HH}$ = 3.3 Hz, 1H, C*H*), 4.75 (d, $^2J_{HH}$ = 10.7 Hz, 1H, CH_2), 4.60 (d, $^2J_{HH}$ = 10.7 Hz, 1H, CH_2), 3.71 (s, 3H, OCH_3), 3.57 (s, 3H, OCH_3). ^{13}C NMR (101 MHz, DMSO–d_6) δ_C 165.2, 159.1, 152.6, 146.5, 136.3, 127.9 (2C), 114.4 (2C), 102.2, 55.5, 53.5, 51.9, 36.6. ESI-HRMS (*m/z*) calculated for $C_{14}H_{16}ClN_2O_4$: 311.0798, found: 311.0820 $[M + H]^+$.

Methyl 6-(chloromethyl)−4-(4-methoxyphenyl)−1-methyl-2-oxo-1,2,3,4-tetrahydropyrimidine-5-carboxylate (**4f**): White crystals, Yield 85.6%. m.p. 174–177 °C. FT-IR: ν (cm^{-1}) = 3414 (N–H), 1682 (*C* = *O*, ester), 1616 (*C* = *O*, amide). ^{1}H NMR (300 MHz, $CDCl_3$) δ_H 7.16 (d, $^3J_{HH}$ = 8.4 Hz, 2H, Ar*H*), 6.83 (d, $^3J_{HH}$ = 8.4 Hz, 2H, Ar*H*), 5.79 (d, $^3J_{HH}$ = 3.2 Hz, 1H, N*H*), 5.34 (d, $^3J_{HH}$ = 3.1 Hz, 1H, C*H*), 4.96 (d, $^2J_{HH}$ = 11.7 Hz, 1H, CH_2), 4.91 (d, $^2J_{HH}$ = 11.9 Hz, 1H, CH_2), 3.78 (s, 3H, OCH_3), 3.69 (s, 3H, OCH_3), 3.38 (s, 3H, NCH_3). ^{13}C NMR (101 MHz, $CDCl_3$) δ_C 165.3, 159.4, 153.7, 146.5, 134.6, 127.5(2C), 114.2 (2C), 106.8, 55.3, 53.1, 51.9, 37.5, 29.4. ESI-HRMS (*m/z*) calculated for $C_{15}H_{18}ClN_2O_4$: 325.0955, found: 325.0961 $[M + H]^+$.

Methyl 6-(chloromethyl)−4-(4-fluorophenyl)−2-oxo-1,2,3,4-tetrahydropyrimidine-5-carboxylate (4 g) White solid, Yield 79.9%. m.p. 182–184 °C. FT-IR: ν (cm^{-1}) = 3234 (N–H), 1691 (*C* = *O*, ester), 1645 (*C* = *O*, amide). ^{1}H NMR (300 MHz, DMSO–d_6) δ_H 9.55 (s, 1H, N*H*), 7.87 (d, $^3J_{HH}$ = 3.4 Hz, 1H, N*H*), 7.28 (dd, $^3J_{HH}$ = 8.6, $^4J_{HF}$ = 5.5 Hz, 2H, Ar*H*), 7.16 (t, $^3J_{HH,HF}$ = 8.8 Hz, 2H, Ar*H*), 5.21 (d, $^3J_{HH}$ = 3.4 Hz, 1H, C*H*), 4.77 (d, $^2J_{HH}$ = 10.8 Hz, 1H, CH_2), 4.58 (d, $^2J_{HH}$ = 10.8 Hz, 1H, CH_2), 3.57 (s, 3H, OCH_3). ^{13}C NMR (75 MHz, DMSO–d_6) δ_C 165.1, 162.0 (d, $^1J_{CF}$ = 243.6 Hz), 152.5, 146.8, 140.4 (d, $^4J_{CF}$ = 3.0 Hz), 128.7 (2C, d, $^3J_{CF}$ = 8.3 Hz), 115.9 (2C, d, $^2J_{CF}$ = 21.5 Hz), 101.9, 53.5, 52.0 (d, $^2J_{CN}$ = 4.10 Hz), 39.7.

Methyl 6-(chloromethyl)−4-(4-fluorophenyl)−1-methyl-2-oxo-1,2,3,4-tetrahydropyrimidine-5-carboxylate (4 h) White solid, Yield 87.2%. m.p. 139.142 °C. FT-IR: ν (cm^{-1}) = 3285 (N–H), 1681 (*C* = *O*, ester), 1655 (*C* = *O*, amide). ^{1}H NMR (300 MHz, $CDCl_3$) δ_H 7.21 (dd, $^3J_{HH}$ = 8.6, $^4J_{HF}$ 5.3 Hz, 2H, Ar*H*), 6.99 (t, $^3J_{HH,HF}$ = 8.7 Hz, 2H, Ar*H*), 5.97 (d, $^3J_{HH}$ = 3.2 Hz, 1H, N*H*), 5.38 (d, $^3J_{HH}$ = 3.4 Hz, 1H, C*H*), 4.98 (d, $^2J_{HH}$ = 11.8 Hz, 1H, CH_2), 4.89 (d, $^2J_{HH}$ = 11.9 Hz, 1H, CH_2), 3.70 (s, 3H, OCH_3), 3.38 (s, 3H, NCH_3). ^{13}C NMR (101 MHz, $CDCl_3$) δ_C 165.1, 162.5 (d, $^1J_{CF}$ = 247.0 Hz), 153.5, 147.0, 138.2 (d, $^4J_{CF}$ = 3.2 Hz), 128.0 (2C, d, $^3J_{CF}$ = 8.2 Hz), 115.9 (2C, d, $^2J_{CF}$ = 21.5 Hz), 106.4, 53.1, 52.0, 37.4, 29.5. ESI-HRMS (*m/z*) calculated for $C_{14}H_{15}ClFN_2O_3$: 313.0755, found: 313.0835 $[M + H]^+$.

4.3. General procedure for the azidation of **4e-h** using **4f** as an example

Sodium azide (2.97 mmol, 0.19 g) was added to dry DMF (55.0 mL) under nitrogen. To this mixture was added a solution of **4e** (2.70 mmol, 0.88 g) in 10.0 mL dry DMF. The resulting mixture was stirred overnight under nitrogen at room temperature. The reaction mixture was poured into distilled water (100.0 mL) and extracted with EtOAc (3 × 25.0 mL). The combined organic layers were washed with brine (25.0 mL) and distilled wa-

ter (5 × 25.0 mL), dried with $MgSO_4$, filtered and concentrated *in vacuo* to give the pure product.

Methyl 6-(azidomethyl)–4-(4-methoxyphenyl)–2-oxo-1,2,3,4-tetrahydropyrimidine-5-carboxylate (**5e**) White solid. Yield 92.7%. m.p. 129–132 °C. FT-IR: ν (cm^{-1}) = 3218 (N–H), 2101 (N_3), 1689 ($C = O$, ester), 1646 ($C = O$, amide). ^{1}H NMR (300 MHz, DMSO–d_6) δ_H 9.43 (s, 1H, N*H*), 7.81 (d, $^3J_{HH}$ = 3.2 Hz, 1H, N*H*), 7.17 (d, $^3J_{HH}$ = 8.6 Hz, 2H, Ar*H*), 6.88 (d, $^3J_{HH}$ = 8.6 Hz, 2H, Ar*H*), 5.15 (d, $^3J_{HH}$ = 3.3 Hz, 1H, C*H*), 4.46 (d, $^2J_{HH}$ = 12.9 Hz, 1H, CH_2), 4.33 (d, $^2J_{HH}$ = 12.9 Hz, 1H, CH_2), 3.71 (s, 3H, OCH_3), 3.57 (s, 3H, OCH_3). ^{13}C NMR (101 MHz, DMSO–d_6): δ_C 165.6, 159.1, 152.4, 144.9, 136.5, 127.9 (2C), 114.3 (2C), 102.7, 55.5, 53.7, 51.8, 48.5. ESI-HRMS (*m/z*) calculated for $C_{14}H_{16}N_5O_4$: 318.1202, found: 318.1245 $[M + H]^+$.

Methyl 6-(azidomethyl)–4-(4-methoxyphenyl)–1-methyl-2-oxo-1,2,3,4-tetrahydropyrimidine-5-carboxylate (**5f**) White crystals,Yield 93.4%. m.p. 128–131 °C. FT-IR: ν (cm^{-1}) = 3202 (N–H), 21,141 (N_3), 1678 ($C = O$, ester), 1627 ($C = O$, amide). ^{1}H NMR (300 MHz, $CDCl_3$) δ_H 7.18 (d, $^3J_{HH}$ = 8.4 Hz, 2H, Ar*H*), 6.84 (d, $^3J_{HH}$ = 8.6 Hz, 2H, Ar*H*), 5.75 (d, $^3J_{HH}$ = 3.2 Hz, 1H, N*H*), 5.37 (d, $^3J_{HH}$ = 3.0 Hz, 1H, C*H*), 4.73 (d, $^2J_{HH}$ = 13.6 Hz, 1H, CH_2), 4.44 (d, $^2J_{HH}$ = 13.6 Hz, 1H, CH_2), 3.78 (s, 3H, OCH_3), 3.69 (s, 3H, OCH_3), 3.28 (s, 3H, NCH_3). ^{13}C NMR (101 MHz, $CDCl_3$) δ_C 165.7, 159.5, 153.5, 144.7, 134.6, 127.5 (2C), 114.2 (2C), 107.9, 55.3, 53.5, 51.9, 46.5, 29.9. ESI-HRMS (*m/z*) calculated for $C_{15}H_{18}N_5O_4$: 332.1359, found: 332.1353 $[M + H]^+$.

Methyl 6-(azidomethyl)–4-(4-fluorophenyl)–2-oxo-1,2,3,4-tetrahydropyrimidine-5-carboxylate (5 g) White crystals, Yield 97.4%. m.p. 136–139 °C. FT-IR: ν (cm^{-1}) = 3226 (N–H), 2098 (N_3), 1694 ($C = O$, ester), 1648 ($C = O$, amide). ^{1}H NMR (300 MHz, DMSO–d_6) δ_H 9.53 (s, 1H, N*H*), 7.91 (d, $^3J_{HH}$ = 3.3 Hz, 1H, N*H*), 7.30 (dd, $^3J_{HH}$ = 8.5, $^4J_{HF}$ = 5.5 Hz, 2H, Ar*H*), 7.18 (t, $^3J_{HH,HF}$ = 8.7 Hz, 2H, Ar*H*), 5.22 (d, $^3J_{HH}$ = 3.3 Hz, 1H, C*H*), 4.49 (d, $^2J_{HH}$ = 12.9 Hz, 1H, CH_2), 4.33 (d, $^2J_{HH}$ = 12.9 Hz, 1H, CH_2), 3.59 (s, 3H, OCH_3). ^{13}C NMR (75 MHz, DMSO–d_6) δ_C 165.5, 162.0 (d, $^1J_{CF}$ = 243.7 Hz), 152.3, 145.3, 140.6 (d, $^4J_{CF}$ = 3.0 Hz), 128.7 (2C, d, $^3J_{CF}$ = 8.3 Hz), 115.8 (2C, d, $^2J_{CF}$ = 21.6 Hz), 102.3, 53.7, 51.9 (d, $^2J_{CN}$ = 5.1 Hz), 48.5. ESI-HRMS (*m/z*) calculated for $C_{13}H_{13}FN_5O_3$: 306.1002, found: 306.1021 $[M + H]^+$.

Methyl 6-(azidomethyl)–4-(4-fluorophenyl)–1-methyl-2-oxo-1,2,3,4-tetrahydropyrimidine-5-carboxylate (5 h) White crystals, Yield 95.6%. m.p. 123–126 °C. FT-IR: ν (cm^{-1}) = 3206 (N–H), 2110 (N_3), 1689 ($C = O$, ester), 1626 ($C = O$, amide). ^{1}H NMR (300 MHz, DMSO–d_6) δ_H 8.16 (d, $^3J_{HH}$ = 3.8 Hz, 1H, N*H*), 7.30 (dd, $^3J_{HH}$ = 8.5, $^4J_{HF}$ 5.5 Hz, 2H, Ar*H*), 7.18 (t, $^3J_{HH,HF}$ = 8.7 Hz, 2H, Ar*H*), 5.22 (d, $^3J_{HH}$ = 3.8 Hz, 1H, C*H*), 4.70 (s, 2H, CH_2), 3.64 (s, 3H, OCH_3), 3.35 (s, 3H, NCH_3). ^{13}C NMR (75 MHz, DMSO–d_6): δ_C 165.9, 162.0 (d, $^1J_{CF}$ = 243.7 Hz), 153.2, 146.4, 139.7 (d, $^4J_{CF}$ = 3.1 Hz), 128.6 (d, $^3J_{CF}$ = 8.3 Hz, 2C), 115.9 (d, $^2J_{CF}$ = 21.3 Hz, 2C), 106.5, 52.3, 52.2, 46.6, 29.8. ESI-HRMS (*m/z*) calculated for $C_{14}H_{15}FN_5O_3$: 320.1159, found: 320.1142 $[M + H]^+$.

4.4. X-ray crystallography

Single crystal diffraction experiments of compounds **4a, 4c, 4d, 4f**, 5 g, and 5 h were performed using Quazar multi-layer optics monochromated Mo Kα radiation (k = 0.71069 Å) on a Bruker D8 Venture kappa geometry diffractometer with duo Iμs sources, a Photon 100 CMOS detector and APEX III control software [30]. Data reduction was performed using SAINT+ [30], and the intensities were corrected for absorption using SADABS [30]. Single crystals of **4b** and **5f** were analysed on a Rigaku XtaLAB Synergy R diffractometer, with a rotating-anode X-ray source and a HyPix CCD detector. Data reduction and absorption were carried out using the CrysAlisPro (version 1.171.40.23a) software package [31]. All X-ray diffraction measurements were performed at 150(1) K, using an Oxford Cryogenics Cryostat. All structures were solved by direct methods with SHELXS-2013 [32] using the OLEX2 [33] interface. All H atoms were placed in geometrically idealised positions and constrained to ride on their parent atoms. For data collection and refinement parameters, see the SI (**Tables S1**-**S3**). The X-ray crystallographic coordinates for all structures have been deposited at the Cambridge Crystallographic Data Centre (CCDC), with deposition numbers CCDC 1,980,412–1,980,419. The data can be obtained free of charge from The Cambridge Crystallographic Data Centre *via*www.ccdc.cam.ac.uk/data_request/cif.

4.5. Computational chemistry methods

All calculations were carried out using Density Functional Theory (DFT) using the B3LYP-D3 (B3LYP with the Grimme empirical dispersion correction D3) hybrid functional [34,35], as implemented in the Gaussian 09 package [36]. The triple-ζ basis set def2-TZVPP [37] was used for all atoms (C, H, N, O, F, Cl). The geometries of all compounds were fully optimised without any symmetry restrictions, ensuring that the local minima had zero imaginary vibrational frequencies and to provide the thermal correction to free energies at 298.15 K and 1 atm. All calculations were performed in either chloroform (ε = 4.71) or DMSO (ε = 46.83) as solvents and corresponds to the solvent that a specific compound was dissolved in as part of the NMR studies. Simulated NMR spectra were calculated using the same level of theory and respective implicit solvent model using the GIAO method [38]. The relative ^{1}H and ^{13}C chemical shifts (δ_H, δ_C) were estimated by using the corresponding TMS shielding calculated at the same level of theory and again using the same implicit solvent model. The implicit solvent Polarizable Continuum Model (PCM) [39] that uses the integral equation formalism variant (IEFPCM) [40] was used for solvent calculations in Gaussian. All energies used and reported in this work are zero point vibrational-corrected.

Declaration of Competing Interest

The authors declare that they have no known competing financial interests or personal relationships that could have appeared to influence the work reported in this paper.

CRediT authorship contribution statement

Rasheed A. Adigun: Conceptualization, Methodology, Formal analysis, Investigation, Writing - review & editing, Data curation. **Frederick P. Malan:** Data curation, Software, Writing - review & editing. **Mohammed O. Balogun:** Supervision, Writing - review & editing. **Natasha October:** Supervision, Project administration, Resources, Funding acquisition, Writing - review & editing.

Acknowledgements

We are grateful to the National Research Foundation (South Africa) (Grant number: 105152) and the University of Pretoria, South Africa for their financial support. We thank Prof Liezel van der Merwe of the Department of Chemistry, University of Pretoria and Dr Jubril Olayinka Akolade of the Council for Scientific and Industrial Research, South Africa, for the DSC and TGA analyses.

Supplementary materials

Supplementary material associated with this article can be found, in the online version, at doi:10.1016/j.molstruc.2020.129193.

References

[1] D.B. Zlatković, N.S. Radulović, Reduction of Biginelli compounds by LiAlH4: a rapid access to molecular diversity, RSC Adv 6 (2016) 115058–115067, doi:10.1039/c6ra24535h.

[2] K.S. Atwal, B.N. Swanson, S.E. Unger, D.M. Floyd, S. Moreland, A. Hedberg, B.C.O. Reilly, Dihydropyrimidine Calcium Channel Blockers. 3.' 3-Carbamoyl-4-aryl-1,2,3,4-tetrahydro-6-methyl-5-pyrimidinecarboxylic Acid Esters as Orally Effective Antihypertensive Agents, J. Med. Chem. 34 (1991) 806–811.

[3] G.C. Rovnyak, K.S. Atwal, S.D. Kimball, B.C. O'Reilly, J. Schwartz, A. Hedberg, S. Moreland, J.Z. Gougoutas, M.F. Malley, Dihydropyrimidine Calcium Channel Blockers, 4. Basic 3-Substituted-4-aryl-1,4-dihydropyrimidine-5-Carboxylic Acid Esters. Potent Antihypertensive Agents, J. Med. Chem. 35 (1992) 3254–3263, doi:10.1021/jm00095a023.

[4] C. Oliver Kappe, 100 Years of the Biginelli Dihydropyrimidine Synthesis, Tetrahedron 49 (1993) 6937–6963 10.1016/S0040-4020(01)87971-0.

[5] K.S. Atwal, G.C. Rovnyak, J. Schwartz, S. Moreland, A. Hedberg, J.Z. Gougoutas, M.F. Malley, D.M. Floyd, Dihydropyrimidine Calcium Channel Blockers: 2-Heterosubstituted 4-Aryl-l,4-dihydro-6-methyl-5-pyrimidinecarboxylic Acid Esters as Potent Mimics of Dihydropyridines, J. Med. Chem. 33 (1990) 1510–1515, doi:10.1021/jm00167a035.

[6] L. Weber, The Application of Multi-Component Reactions in Drug Discovery, Curr. Med. Chem. 9 (2002) 2085–2093, doi:10.2174/0929867023368719.

[7] L. Weber, Multi-component reactions and evolutionary chemistry, Drug Discov. Today. 7 (2002) 143–147 10.1016/S1359-6446(01)02090-6.

[8] E. Black, R. Richmond, Improving early detection of breast cancer in sub-Saharan Africa: why mammography may not be the way forward, Global. Health 15 (2019) 3.

[9] A.R. Jazieh, A. Bounedjar, F. Al Dayel, S. Fahem, A. Tfayli, K. Rasul, H. Jaafar, M. Jaloudi, T. Al Fayea, H.Q. Al Maghrabi, The Study of Druggable Targets in Nonsquamous Non-Small-Cell Lung Cancer in the Middle East and North Africa, J. Immunother. Precis. Oncol. 2 (2019) 4.

[10] K.A. Twohig, D.A. Pfeffer, J.K. Baird, R.N. Price, P.A. Zimmerman, S.I. Hay, P.W. Gething, K.E. Battle, R.E. Howes, Growing evidence of Plasmodium vivax across malaria-endemic Africa, PLoS Negl. Trop. Dis 13 (2019) e0007140.

[11] M.K. Kushitor, S. Boatemaa, The double burden of disease and the challenge of health access: evidence from Access, Bottlenecks, Cost and Equity facility survey in Ghana, PLoS ONE 13 (2018) e0194677, doi:10.1371/journal.pone.0194677.

[12] A. Gessner, J. König, M.F. Fromm, Clinical Aspects of Transporter-Mediated Drug-Drug Interactions, Clin. Pharmacol. Ther (2019).

[13] S.Mishra Shaveta, Singh Palwinder, Hybrid molecules: the privileged scaffolds for various pharmaceuticals, Eur. J. Med. Chem 124 (2016) 500–536, doi:10.1016/j.ejmech.2016.08.039.

[14] M.S. Malik, Z.S. Seddigi, S. Bajee, S. Azeeza, S. Riyaz, S.A. Ahmed, I.I. Althagafi, Q.M.S. Jamal, A. Kamal, Multicomponent access to novel proline/cyclized cysteine tethered monastrol conjugates as potential anticancer agents, J. Saudi Chem. Soc. 23 (2019) 503–513.

[15] T. Chiba, H. Sato, T. Kato, Synthesis of furo [3, 4-d] pyrimidine derivatives using ethyl 4-bromoacetoacetate, Heterocycles (Sendai) 22 (1984) 493–496.

[16] R. Pérez, T. Beryozkina, O.I. Zbruyev, W. Haas, C.O. Kappe, Traceless Solid-Phase Synthesis of Bicyclic Dihydropyrimidones Using Multidirectional Cyclization Cleavage, J. Comb. Chem. 4 (2002) 501–510, doi:10.1021/cc0200181.

[17] F.A.R. Barbosa, R.F.S. Canto, S. Saba, J. Rafique, A.L. Braga, Synthesis and evaluation of dihydropyrimidinone-derived selenoesters as multi-targeted directed compounds against Alzheimer's disease, Bioorganic Med. Chem. 24 (2016) 5762–5770, doi:10.1016/j.bmc.2016.09.031.

[18] R.J. Anderson, D.J. Bendell, P.W. Groundwater, Organic Spectroscopic Analysis, Royal Society of Chemistry (2007), doi:10.1039/9781847551566.

[19] L.Pavia Donald, G.M. Lampman, G.S. Kriz, J.R. Vyvyan, Introduction to Spectroscopy, 5th ed., Cengage Learning, 2015.

[20] P.S. Lebed', P.O. Kos, V.V. Polovinko, A.A. Tolmachev, M.V. Vovk, Synthesis of new polyfunctional 5,6,7,8-tetrahydroimidazo-[1,5-*c*]pyrimidin-5-ones by the aza-Wittig reaction followed by intramolecular cyclization and 1,3-prototropic shift, Russ. J. Org. Chem. 45 (2009) 921–927, doi:10.1134/S1070428009060207.

[21] A.S. Mostafa, K.B. Selim, Synthesis and anticancer activity of new dihydropyrimidinone derivatives, Eur. J. Med. Chem. 156 (2018) 304–315, doi:10.1016/j.ejmech.2018.07.004.

[22] B. Khanetskyy, D. Dallinger, C.O. Kappe, Combining Biginelli Multicomponent, Click Chemistry, Generation of 6-(1,2,3-Triazol-1-yl)-Dihydropyrimidone Libraries, J. Comb. Chem. 6 (2004) 884–892, doi:10.1021/cc0498938.

[23] C.O. Kappe, Unexpected Formation of Nitriles from Reactions of 6-(Dibromomethy1)- 1,2,3,4-tetrahydro-2-oxo-5-pyrimidinecarboxylates with Sodium Azide, Liebigs Ann. Der Chemie. 5 (1990) 505–507.

[24] Proton Chemical Shifts, (n.d.). https://www.chem.wisc.edu/areas/reich/nmr/h-data/hdata.htm (accessed June 11, 2019).

[25] A. Dhandapani, S. Manivarman, S. Subashchandrabose, Synthesis, single crystal structure, Hirshfeld surface and theoretical investigations on pyrimidine derivative, Chem. Phys. Lett. 655–656 (2016) 17–29, doi:10.1016/j.cplett.2016.04.009.

[26] S. Bharanidharan, H. Saleem, B. Gunasekaran, M.S.A. Padusha, M. Suresh, Crystal structure of ethyl 6-(chloromethyl)-4-(4-chlorophenyl)-2-oxo-1,2,3,4-tetrahydropyrimidine-5-carboxylate, Acta Crystallogr. Sect. E Struct. Reports Online. 70 (2014) o1185–o1186, doi:10.1107/S1600536814023046.

[27] R.A. Adigun, F.P. Malan, M.O. Balogun, N. October, Tetrahydropyrimidinones/thiones stabilized by trifluoromethyl-containing β-diketones„ J. Mol. Struct. 1202 (2019) 127281, doi:10.1016/j.molstruc.2019.127281.

[28] B. Lagu, D. Tian, G. Chiu, D. Nagarathnam, J. Fang, Q. Shen, C. Forray, R.W. Ransom, R.S.L. Chang, K.P. Vyas, K. Zhang, C. Gluchowski, Synthesis and evaluation of furo[3,4-*d*]pyrimidinones as selective α(1a)-adrenergic receptor antagonists, Bioorg. Med. Chem. Lett. 10 (2000) 175–178 10.1016/S0960-894X(99)00653-8.

[29] S.K. Mohamed, A.M. Soliman, M.A.A. El Remaily, H. Abdel-Ghany, Rapidly and Highly Yielded Synthesis of Pyrimidine, Dihydropyrimidinone, and Triazino[2,1-*b*]quinazolin-6-ones Derivatives, J. Heterocycl. Chem. 50 (2013) 1425–1430, doi:10.1002/jhet.

[30] APEX3(including SAINT and SADABS), Bruker AXS Inc., Madison, WI, 2016.

[31] Rigaku Oxford Diffraction, CrysAlisPro Software system, (2018).

[32] G.M. Sheldrick, SHELXT - Integrated space-group and crystal-structure determination, Acta Crystallogr. Sect. A Found. Adv A71 (2015) 3–8, doi:10.1107/S2053273314026370.

[33] O.V. Dolomanov, L.J. Bourhis, R.J. Gildea, J.A.K. Howard, H. Puschmann, OLEX2: a complete structure solution, refinement and analysis program, J. Appl. Crystallogr. 42 (2009) 339–341.

[34] A.D. Becke, Becke's three parameter hybrid method using the LYP correlation functional, J. Chem. Phys. 98 (1993) 5648–5652.

[35] C. Lee, W. Yang, R.G. Parr, Development of the Colle-Salvetti conelation energy formula into a functional of the electron densityâ€™, Phys. Rev, Vol. B. 37 (1988) 785–789.

[36] M.J. Frisch, G.W. Trucks, H.B. Schlegel, G.E. Scuseria, M.A. Robb, J.R. Cheeseman, G. Scalmani, V. Barone, B. Mennucci, G.A. Petersson, GAUSSIAN 09, Rev. C. 01, D. 01, Gaussian, Wallingford CT, 2010.

[37] F. Weigend, R. Ahlrichs, Balanced basis sets of split valence, triple zeta valence and quadruple zeta valence quality for H to Rn: design and assessment of accuracy, Phys. Chem. Chem. Phys. 7 (2005) 3297–3305 10. 1039/B508541A.

[38] J.R. Cheeseman, G.W. Trucks, T.A. Keith, M.J. Frisch, A Comparison of Models for Calculating Nuclear Magnetic Resonance Shielding Tensors, J. Chem. Phys. 104 (1996) 5497–5509, doi:10.1063/1.471789.

[39] A.V. Marenich, C.J. Cramer, D.G. Truhlar, Universal solvation model based on solute electron density and on a continuum model of the solvent defined by the bulk dielectric constant and atomic surface tensions, J, Phys. Chem. B 113 (2009) 6378–6396.

[40] R.E. Skyner, J.L. Mcdonagh, C.R. Groom, T. Van Mourik, A review of methods for the calculation of solution free energies and the modelling of systems in solution, Phys. Chem. Chem. Phys. 17 (2015) 6174–6191, doi:10.1039/C5CP00288E.